Islet amyloid polypeptide triggers limited complement activation and binds complement inhibitor C4b-binding protein, which enhances fibril formation.

Sjölander, Jonatan; Westermark, Gunilla T; Renström, Erik; Blom, Anna

Published in:
Journal of Biological Chemistry

DOI:
10.1074/jbc.M111.244285

2012

Islet amyloid polypeptide triggers limited complement activation and binds complement inhibitor C4b-binding protein, which enhances fibril formation.

Jonatan Sjölander[1], Gunilla T. Westermark[2], Erik Renström[3], Anna M. Blom[1, *]

From [1]Department of Laboratory Medicine, Lund University, Wallenberg Laboratory, Skåne University Hospital, S-20502 Malmö, Sweden;

[2]Department of Medical Cell Biology, Uppsala University, S-75123 Uppsala, Sweden

[3]Department of Clinical Sciences, Islet Pathophysiology, Lund University, Clinical Research Centre, Skåne University Hospital, S-20502 Malmö, Sweden

Running tile: IAPP and complement

Address correspondence to: Anna Blom, Prof, Lund University, Dept. of Laboratory Medicine, Section of Medical Protein Chemistry, University Hospital, Malmö, S-20502 Malmö, Sweden. Tel: 46-40-338233; Fax: 46-40-337043; E-mail: anna.blom@med.lu.se

Islet amyloid polypeptide (IAPP) is synthesized in pancreatic β-cells and co-secreted with insulin. Aggregation and formation of IAPP-amyloid plays a critical role in β-cell death in type 2 diabetic patients. Since Aβ-fibrils in Alzheimer's disease activate the complement system, we have here investigated specific interactions between IAPP and complement factors. IAPP fibrils triggered limited activation of complement *in vitro*, involving both the classical and the alternative pathways. Direct binding assays confirmed that IAPP fibrils interact with globular head domains of complement initiator C1q. Furthermore, IAPP also bound complement inhibitors factor H and C4b-binding protein (C4BP). Recombinant C4BP mutants were used to show that complement control protein (CCP) domains 8 and 2 of the α-chain were responsible for the strong, hydrophobic binding of C4BP to IAPP. Immunostaining of pancreatic sections from type 2 diabetic patients revealed the presence of complement factors in the islets and varying degree of co-localization between IAPP fibrils and C1q, C3d as well as C4BP and FH but not membrane attack complex. Furthermore, C4BP enhanced formation of IAPP fibrils *in vitro*. We conclude that C4BP binds to IAPP thereby limiting complement activation and may be enhancing formation of IAPP fibrils from cytotoxic oligomers.

Deposition of amyloid is one of the main pathological characteristics in patients with type 2 diabetes (T2D). These amyloid deposits were first named islet amyloid because of its location inside the islets of Langerhans and later found to consist of the polypeptide hormone, islet amyloid polypeptide (IAPP) (1), which is expressed by the β-cell and co-secreted together with insulin (2,3). A reduction in β-cell number is observed in patients with T2D (4) and the severity of the disease has been suggested to correlate with the amount of IAPP amyloid (5-7). IAPP fibrils are made of several interacting protofilaments. Each protofilament consists of numerous vertical monomers, which are stacked on top of each other, forming an elongated β-sheet. Formation of amyloid fibrils includes the assembly of smaller intermediates referred to as oligomers (8). Amyloid has been shown to induce apoptosis (9) but the exact cytotoxic conformation remains a matter of debate. Oligomers have the ability to incorporate into membranes and form ion leaking pores (10), which may be the reason for their cytotoxicity. In this scenario, mature amyloid fibrils appear to be a way to safely neutralize toxic oligomers. However, the existence of IAPP oligomers *in vivo* is still under debate (11).

The complement system is a pivotal component of innate immunity. Besides its classical functions such as opsonisation of pathogens, generation of inflammatory mediators and cell lysis, its roles in the recognition and removal of dying cells, immune complexes and misfolded proteins are of significant importance (12). IAPP has been suggested to activate complement (13) and therefore, interactions between complement and IAPP can be of importance for the normal islet physiology, but also for the development of pathologic deposits present in the islets of patients with T2D. The complement cascade is organized in three pathways of which the classical route is triggered by C1 complex binding to immune complexes causing activation of C4 and C2, which together form the classical C3-convertase (14). The C1 complex is composed of two proteases C1s and

C1r as well as C1q, which recognizes a number of molecules such as immune complexes, C-reactive protein and misfolded proteins (15). C1q is also present in a free form in tissues and in plasma (10% of total amount) (16). Spontaneous hydrolysis of C3 or binding of properdin lead to activation of the alternative pathway (17). The lectin pathway is prompted when mannose-binding lectin (MBL) or ficolins bind carbohydrates present on microbial surfaces. The three pathways converge at the level of C3b, which is followed by formation of the C5-convertase, release of the anaphylatoxin C5a and assembly of the membrane attack complex (18).

If complement was left uncontrolled it would lead to general spontaneous activation with severe tissue damage (12). To prevent this, complement remains under constant control of a number of soluble and membrane-bound inhibitors. The main function for C4b-binding protein (C4BP) is to inhibit the classical and lectin pathways, while factor H (FH) controls the alternative pathway. C4BP and FH circulate in blood and act on the level of C3/C5 convertases (14) and both inhibitors contain complement control protein (CCP) domains. C4BP is a 570 kDa protein composed of six identical α-chains and a unique β-chain consisting of eight and four CCP domains, respectively (19). The majority of C4BP molecules in the blood circulate in a high affinity complex with protein S bound to CCP1 of the β-chain (20). We have previously shown that C4BP interacts with amyloid fibrils formed by amyloid-β (Aβ) in Alzheimer's disease and prions (21,22). Under some pathological conditions complement activation can be either excessive or misdirected and contribute to tissue damage (23). The aim of the present study was to elucidate the interactions between complement factors and IAPP fibrils in relation to T2D.

Experimental Procedures

Proteins- C4BP (24), FH (25), C1q (26) were purified from human plasma as described while MBL was purchased from State Serum Institute, Denmark. C1 complex and properdin were purchased from Complement Technology (Tyler TX, USA). C1q tail and globular head domains were prepared using partial proteolytic digestion of C1q with pepsin (Worthington Biochemical, Lakewood, USA) or collagenase from *Clostridium histolyticum* (Worthington Biochemical), respectively (27,28). Recombinant wild type (wt) C4BP and mutants lacking individual CCP domains were expressed in eukaryotic cells and purified by affinity chromatography as described (29). The core fragment of C4BP was obtained by limited digestion with chymotrypsin leaving only the C-terminal extension of the α-chains together with the CCP8 and a truncated CCP7 (30). Human mature processed full-length IAPP (amino acids 1-37) was purchased from Keck Biotechnology (Yale University, New Haven, CT, USA) and Bachem (Bubendorf, Switzerland). Human IAPP fragment composed of amino acids 20-29 (20-29 IAPP), which is the part of the molecule that contains one of the amyloidogenic sequences of human IAPP as well as non-amyloidogenic rat IAPP were purchased from Bachem (31). Human IAPP was amidated at C-terminus while the 20-29 IAPP had a free C-terminus. IAPP peptides and Aβ (amino acids 1-42; Bachem) were dissolved in DMSO and 0.1% NH_3, respectively. All peptides were aliquoted and stored at -80°C, until used except for the aliquot of IAPP used for Tht experiment, which was stored in DMSO up to several weeks at RT. To obtain fibrils, IAPP peptides were diluted with water to a final concentration of 100 μg/ml and 1% in DMSO and incubated for at least 2 days in glass tubes at RT. Aβ formed fibrils already after 1h incubation at RT in 0.1% NH_3. The presence of fibrils was verified with transmission electron microscopy after negative staining. Furthermore, we also performed several experiments crucial for this study using fibrils formed for more prolonged times (up to weeks) with the same results.

Direct Binding Assays - Microtiter plates (Maxisorp, Nunc, Roskilde, Denmark) were coated overnight at 4°C or 2 h in 37°C with 50 μl of 1% w/v BSA (Sigma, S:t Louis, USA; negative control), 5 μg/ml Aβ (positive control), full length human IAPP, 20-29 IAPP or rat IAPP diluted in coating buffer (75 mM sodium carbonate buffer, pH 9.6). For C1q head/tail binding to IAPP 10 μg/ml C1q heads and tails were coated to the bottom of the well as well as BSA. All proteins except rat IAPP, C1q and BSA formed fibrils (32) before coating them onto the plate. The wells were then washed extensively with washing buffer (50 mM Tris-HCl, 150 mM NaCl, 0.1% (v/v)

Tween 20, pH 7.5) followed by 2 h incubation at RT with blocking solution, 1% BSA in PBS or 3% fish gelatin (Norland Products, Cranbury, NJ, USA) in washing buffer. Purified C1q, C1, MBL, properdin, IAPP FH and C4BP at concentrations ranging between 0.5 μg/ml and 50 μg/ml in binding buffer (50 mM HEPES, pH 7.4, 100 mM NaCl, 2 mM $CaCl_2$, 50 μg/ml BSA) were added to the wells and left to incubate for 1 h at 37°C or 4°C overnight. For experiments assessing ionic strength dependency, increasing amounts of NaCl were added to the binding buffer. Specific polyclonal antibodies, rabbit anti IAPP 1:4000 (Abcam, Cambridge, United Kingdom), rabbit anti-human C1q (Dako, Glostrup, Denmark) diluted 1:6000, goat anti-human FH (Quidel, San Diego, CA, USA) diluted 1:2000, rabbit anti-C4BP (made in house) 3.25 μg/ml of purified IgG fraction, goat anti MBL (R&D, Minneapolis, MN USA) 1:2000 were diluted in blocking solution and incubated for 1 h at RT. This was followed by incubation with swine anti-rabbit IgG (Dako) or rabbit anti-goat IgG (Dako) conjugated with horseradish peroxidase (HRP), diluted 1:2000 in a blocking solution. Bound enzyme was visualized using the 1,2-phenylenediamine dihydrochloride (OPD)/H_2O_2 colorimetric substrate (Dako). The reaction was terminated with 0.5 M H_2SO_4 and the absorbance was measured at 490 nm in a plate reader (Varian, Palo Alto CA, USA). The binding assays were repeated with the same result when PBS instead of carbonate buffer was used as coating solution.

Complement activation assays - Microtiter plates were incubated overnight at 4°C with 50 μl of the coating buffer containing 5 μg/ml of Aβ, full length human IAPP, rat IAPP, 20-29 IAPP, 2 μg/ml human aggregated IgG (Immuno, Vienna, Austria) or 1% BSA. The amyloidgenic proteins were coated onto the plates as fibrils. Between each incubation step, the plates were washed four times with washing buffer. The wells were blocked with blocking solution for 1 h at RT. Normal human serum (NHS) was prepared and pooled from blood taken from six healthy donors as approved by the ethical committee of Lund University. Dilutions of NHS in GVB^{++} (2.5 mM veronal buffer pH 7.3, 150 mM NaCl, 0.1% gelatin, 1 mM $MgCl_2$ and 0.15 mM $CaCl_2$) or Mg++ EGTA buffer (2.5 mM Veronal buffer, oh 7.3, 70 mM NaCl 140 mM glucose, 0.1% gelatin,7mM $MgCl_2$, 10 mM EGTA) were added to the wells and incubated for 20 min (for detection of C1q, C3b and C4b) or 45 min (C9), at 37°C, followed by incubation with specific rabbit polyclonal antibodies against C1q (Dako) diluted 1:6000, C3d (Dako) diluted 1:2000, C4b (Dako) diluted 1:2000, FH (Quidel) diluted 1:6000 or goat polyclonal antibodies against C9 (Complement Technology) diluted 1:2000. All antisera were diluted in blocking solution. HRP-conjugated secondary antibodies swine anti-rabbit IgG (Dako) or rabbit anti-goat IgG (Dako), where both diluted 1:2000 in blocking solution. Bound HRP was measured using the colorimetric assay as described above for the direct binding assay.

Electron microscopy – An aliquot of 15 μl samples of Aβ, full length IAPP, IAPP 20-29 fibrils or rat IAPP with the protein concentration of 100 μg/ml or 15 μl of sample from thioflavin T (Tht) experiment after incubation for various time points and containing IAPP alone or IAPP with highest concentration of C4BP tested were placed on formvar coated copper grids (Link, Nordic Analytical, Lidingö, Sweden) and incubated for 30 s. The peptide solution was then replaced by 2% uranyl acetate (Link) in 50% ethanol. The fibrils were studied at 100 kV in a Jeol 1230 electron microscope (Jeol, Akishima, Japan). Electron micrographs were taken with a Gatan multiscan camera model 791 using Gatan digital software version 3.6.4 (Gatan, Pleasanton, USA).

Fluorescence microscopy – sections of pancreas from patients with T2D were used to visualize complement factors in the islets. The tissue material has been anonymized and the ethical board at Uppsala University has approved its use in research. Formalin-fixed paraffin embedded sections were mounted on glass slides and deparaffinized in xylene for 2 x 10 min, rehydrated with decreasing percentage of ethanol and distilled water. Antigen retrieval was performed to expose epitopes by incubation in 0.01 M Na-citrate buffer pH 6.0, at 99 °C for 20 minutes for the exception of C4BP staining where the antigen recovery heating only lasted 1 min. All sections were rinsed 3 times with 0.05 M Tris with 0.15 M NaCl, pH 7.4 (TBS) and incubated with primary antibodies overnight at 4°C. The following antibodies were included; goat anti-

FH (Quidel) diluted 1:250, affinity purified rabbit anti-C4BP (13 μg/ml), rabbit anti-C1q (Dako) diluted 1:125, rabbit anti-C3d (Dako) diluted 1:250 or rabbit anti-SC5b-9 (Complement Technology) diluted 1:250. The formalin fixed sections were also incubated with a mouse anti-IAPP antibody (Abcam) diluted 1:100. The antibody binds aa 7-17 of processed mature human IAPP thus recognizing IAPP in intracellular insulin granules, intracellular amyloid and extracellular islet amyloid. After washing in TBS the sections were incubated for 3 h at RT with Alexa Fluor 488 labeled secondary antibodies (Molecular Probes, Eugene Ore, USA) diluted 1:1000 in TBS. IAPP reactivity was visualized with Alexa Fluor 647 (Molecular Probes) diluted 1:1000 in TBS for 3 h at RT. Some of the sections were also stained for amyloid with Congo red (Sigma) as described (33). The paraffin sections were analysed on a Zeiss LCM 510 confocal microscope. All images are representative of at least three independent staining experiments. Co-localization was calculated using CoLocalizer Pro (CoLocalization Research Software) and three representative images acquired independently for each staining (34).

Thioflavin T assay – A kinetic study of amyloid fibril formation was carried out in black 96-well plates (Nunc). Full-length IAPP (Keck) was diluted from a stock of 20 mg/ml IAPP in DMSO (kept at RT) to a final concentration of 17 μg/ml in 50 mM glycine, 25 mM sodium phosphate buffer, pH 7.0 yielding a final concentration of 0.3% DMSO. C4BP dialyzed against the same buffer or BSA (10 mg/ml, negative control) were also added to the wells to final concentrations ranging from 0-300 μg/ml followed by 10 μM Tht (Sigma). Excitation was set to 442 nm and emission to 482 nm and the fluorescence was measured every 10 minutes for 16 hours using an Infinity 200 microplate reader equipped with a Quad4 monochromator (Tecan, Männedorf, Switzerland).

Statistical Analysis - Student's *t* test for unpaired samples, two-way ANOVA with Bonferroni and one-way ANOVA with Tukey's multiple comparison test were used to evaluate statistical significance of differences between groups (GraphPad Software); *, $p < 0.05$; **, $p < 0.01$; ***, $p < 0.001$.

RESULTS

Complement factors C1q, C3d, C5b-9 and complement inhibitors C4BP and FH co-localize to various extents with IAPP and IAPP fibrils in human pancreatic tissue. Since human IAPP was reported to trigger complement activation via the classical pathway (13), amyloid-containing pancreatic sections from patients with T2D were stained for complement components. The colocalization was quantified using ColocalizerPro software. Confocal microscopy analysis revealed co-localization of C1q (Fig. 1A), C3d (Fig. 1B) and C5b-9 complexes (component of MAC; Fig. 1C) as well as inhibitors C4BP (Fig. 1D) and FH (Sup. 1D) with IAPP visualized with monoclonal antibody detecting all forms of intra and extracellular IAPP (Fig. 1A-D). Amyloid detected with Congo red staining was also labeled to various extent by C1q, C3d, C5b-9, C4BP (Fig. 1E-I) and FH (Sup. 1E) specific antibodies, and merged overlapping pixels where visualized as white using the ColocalizerPro software. Quantitative analyses of co-localisation yielded overlap coefficients according to Manders (R; Table 1). R indicates an actual overlap of the two signals and is considered to represent true colocalisation. All studied complement proteins showed significant colocalisation with IAPP but only C3d and C4BP co-localized to a high degree with mature fibrils. This indicates that FH and MAC are present in the islets but not exclusively bound to the mature IAPP fibrils. Results obtained for C1q varied between deposits within the same pancreatic section, some islets showing almost no colocalisation with IAPP fibrils (R = 0.2, Fig. 1F) while others had a high degree of such colocalisation (R = 0.72, Fig. 1E). The studied complement proteins were largely limited to islets and blood vessels, with the exception of FH and that were also weakly detectable in the exocrine pancreas.

Aβ, full-length human IAPP and 20-29 IAPP form fibrils in contrast to rat IAPP. Electron microscopy was used to ascertain that the IAPP variants used in this study form fibrils as described previously (31). As previously reported, rat IAPP lacked entirely the ability to form fibrils (not shown). By contrast, Aβ formed extensive fibrils under the experimental conditions used (Fig. 2C). Full length IAPP formed fibrils very similar to Aβ (Fig. 2A) while 20-29 IAPP formed thicker, well-structured fibrils (Fig. 2B).

IAPP binds C1q and activates weakly the classical and alternative pathways of complement in vitro. The histological findings indicated deposition of C3d co-localized with islet amyloid. To investigate the capacity of IAPP to bind C1q and to activate the classical complement cascade *in vitro* we coated microtiter plates with different variants of IAPP and Aβ (positive control (18)), followed by incubation with purified C1q. C1q bound to both Aβ as well as full length IAPP and weakly to rat IAPP and human (20-29) IAPP (Fig. 3A). Furthermore, there was binding of C1q/C1 from NHS to full length IAPP and weak interaction with Aβ (Fig. 3B). The interaction between purified C1q and full length IAPP was based on ionic interactions and decreased with increasing ionic strength of a binding buffer (Fig. 3C). Next, a binding assay using purified components showed that both free C1q and the C1 complex bound IAPP immobilized on microtiter plate (Fig. 3E). Furthermore, IAPP bound head domains but not tail regions of C1q (Fig. 3F). No binding of MBL or ficolins -1 and -3 from NHS to immobilized IAPP could be detected (not shown).

Binding of C1q from NHS to IAPP was rather weak and we therefore used deposition assays detecting consecutive components of the complement cascade to determine the degree of IAPP-mediated complement activation. All IAPP variants as well as Aβ triggered weak but statistically significant C4b deposition (Fig. 4A). In the classical pathway, deposition of C3b (Fig. 4B) as well as the MAC/C9 molecules (Fig. 4C) was detectable, albeit even weaker than that observed for C4b. Furthermore, IAPP caused more C3b deposition than C9 when conditions allowing only activation of the alternative pathway were used (Fig. 4D-E). The observed low degree of activation of the alternative pathway was not due to direct interaction between properdin and IAPP (not shown).

C4BP binds strongly to IAPP in a hydrophobic manner. Deposition of C3b and C9 triggered by IAPP was weaker than that of C4b in the classical pathway. This taken together with the fact that C4BP binds other types of amyloid (22) prompted us to test if it also binds IAPP. Indeed, purified C4BP bound strongly to full length human IAPP and more weakly to rat IAPP and human (20-29) IAPP (Fig. 5A). Aβ and BSA were used as positive and negative controls, respectively. C4BP from NHS bound efficiently to all forms of IAPP (Fig. 5B). The binding was mainly based on hydrophobic interactions since the interaction was enhanced at higher NaCl concentrations (Fig. 5C). No competition for binding to IAPP was found between C4BP and C1q or between C4BP and FH (not shown).

IAPP interacts with CCP2 and CCP8 of C4BP α-chain. To examine which part of the C4BP-PS complex that bound IAPP we used a direct binding assay with a number of C4BP mutants and fragments (Fig. 6A). Recombinant C4BP composed of only 6 α-chains and lacking protein S and the β-chain (25) bound to IAPP comparably efficient to C4BP purified from plasma (Fig. 6B) implying that the binding site of IAPP was localized in the α-chain of C4BP. The binding site was then localized to CCP2 and CCP8 in the C4BP α-chain in assays employing C4BP mutants lacking one CCP domain each. This was further confirmed by the observation that the core fragment of C4BP containing a fragment of CCP7, the whole CCP8 and C-terminal polymerization region also bound IAPP (Fig. 6B).

C4BP enhances fibril formation. To further evaluate the role of C4BP in IAPP amyloidosis we measured the kinetics of fibril formation in the presence of C4BP. To this end we used Tht that undergoes a detectable shift in fluorescence upon interaction with fibrils but not monomers or oligomers of IAPP. Under the conditions used, 75 150 and 300 μg/ml of C4BP yielded significantly higher end point fluorescence (Fig. 7A). Furthermore, addition of 300 μg/ml C4BP resulted in a significantly shorter lag phase. Fitting the data to a sigmoidal dose-response curve and estimating the T50 (time to 50% completion) values between 0 - 900 min validated the above observations. The concentration of 300 μg/ml C4BP gave a lower T50 value (217.0 to 259.2 min within a 95% confidence interval) compared with IAPP alone (291.9 to 329 min within a 95% confidence interval). Fig. 7B shows the dose dependent effect of C4BP on fibril formation at 400 min (Fig. 7B). C4BP alone (in the absence of IAPP) did not affect the fluorescence intensity of Tht (data not shown). BSA showed no enhancement of fibril formation (Fig. 7B), nor did several other plasma proteins tested (data not shown). EM analysis of sample aliquots of Tht experiment verified the effect of C4BP. In the

sample containing IAPP and 300 μg/ml C4BP there were easily detectable fibrils (Fig. 7C) at much earlier time point than in the sample containing IAPP alone. Mature fibrils formed in the presence of C4BP did not differ in morphology from those formed by IAPP alone when analyzed after 960 min. *FH binds to IAPP*. The fact that the deposition of C9 triggered by IAPP was lower than that of C3b in the alternative pathway (Fig. 4D-E) indicated that IAPP may interact with FH. Indeed, purified FH bound weakly to all forms of IAPP and strongly to Aβ (Fig. S1A). FH from NHS bound weakly to all forms of IAPP and Aβ (Fig. S1B). The interaction between FH and IAPP was largely independent of ionic interactions because it was not decreased at higher NaCl concentrations (Fig. S1C). The small increase in binding observed at 2 M NaCl indicated a hydrophobic component in the interaction.

DISCUSSION

Type 2-diabetes is associated with chronic low-grade inflammation (35) and an upregulation of complement factors (36), but the exact triggering mechanism remains unknown. A previous study indicated a certain complement activating potential of IAPP (13) produced and secreted by the pancreatic β-cell. This observation suggested a novel link between T2D and complement, which is particularly important now when pharmacological complement inhibitors are emerging in clinical trials (37).

The aim of the present study was to investigate interactions between complement factors and IAPP fibrils in relation to T2D. Complement activation could contribute to death of β-cells due to assembly of MAC and in addition, fuel local inflammation by releasing anaphylatoxins. The findings from both the *in vitro* deposition assays measuring C1q, C4b, C3d and C9 as well as the tissue stainings (Fig. 1A-H) confirmed such a limited activation of the complement system by IAPP. The peptide was capable of weakly triggering the alternative pathway *in vitro*, which was not attributable to binding of properdin (data not shwon). It is reasonable to presume that the observed IAPP-induced activation of the classical/lectin complement pathway was initiated by the binding of C1 to IAPP, as shown by the *in vitro* binding assay. While we could not detect any interaction with MBL or ficolins from serume we found that the binding of purified C1q to IAPP was significant. The binding of C1q/C1 from NHS to IAPP was rather low and observed only for full length IAPP, which is likely to be explained by the fact that concentration of free C1q is low in NHS while the purified C1 complex only bound weakly to full length IAPP. IAPP bound globular head domains and not C1q tails, which is characteristic of ligands activating C1 complex (15). Thus, C1q appears to interact with a number of distinct amyloid structures such as Aβ-fibrils in Alzheimer's disease with implications for complement activation and macrophage phagocytosis (38). Also amyloid plaques in Down's syndrome (39), familial British dementia and familial Danish dementia (40) bind C1q to form stable complexes. Furthermore, amyloid forming prion proteins also bind and activate C1q (21).

One reason for the observed low level of MAC deposition is the interactions of IAPP with complement inhibitors such as C4BP and FH. Such phenomenon i.e. limitation of complement activation by C4BP and FH on endogenous ligands such as apoptotic cells, C-reactive protein or misfolded proteins has been observed previously (21). FH showed statistically significant but a very weak binding to IAPP while we could demonstrate a strong binding of C4BP to IAPP *in vitro*, both in purified form and from NHS. Using different recombinant deletion mutants of C4BP this hydrophobic interaction could be mapped to the CCP2 and CCP8 domains. This is similar to what we observed previously for the Aβ-C4BP interaction, which is hydrophobic and dependent on CCP7-8 (22). Thus it appears that the binding to amyloid may be a general property of C4BP and not specific for a particular type of amyloid. Importantly, C4BP bound to amyloid can be expected to inhibit complement since the binding sites for C4b and C3b required for complement inhibitory activity of C4BP are localized to CCP1-4 (29). Indeed we have observed previously that this was the case for Aβ (22) and amyloid fibrils of prion protein (21). Importantly, C4BP is a polymer of 7 identical α-chains and therefore contains multiple interaction sites for all ligands that bind α-chains.

To investigate the physiological relevance of the detected interactions between complement and IAPP, we examined

deposition of complement factors and inhibitors in pancreatic tissue from T2D patients using immunostaining. A high degree of co-localization between C4BP and IAPP was observed in pancreas both upon staining of IAPP with antibodies and Congo red confirming the *in vitro* findings obtained using purified proteins and whole serum. However, C4BP co-localized to a larger degree with IAPP amyloid detected with Congo red than with total intra and extracellular IAPP stained with antibody (Fig 1D, H) indicating that C4BP may preferentially be bound to IAPP fibrils. We also observed significant deposits of C1q, C3d, C5b-9 (MAC) and FH in the pancreatic islets, however, only C3d was found to strongly colocalize with the mature Congo red stained IAPP fibrils. MAC showed virtually no colocalisation with IAPP fibrils indicating that C4BP and FH efficiently down regulate IAPP-fibril mediated complement activation *in vivo*. Interestingly high degree of colocalisation was found between MAC and IAPP detected with antibodies implying that MAC components may be expressed by β-cells and colocalize intracellularly with non-fibrillar IAPP. FH showed most widely distributed staining including areas outside pancreatic islets but it was found to colocalize to 48% with IAPP fibrils. Results obtained for C1q varied between deposits within the same pancreatic section with regards to degree of colocalisation with IAPP fibrils. The reason for such diversity is unknown and requires further investigation with larger clinical material. In contrast to C1q, all amyloid-containing islets stained for C3d indicating that in addition to activation of the classical pathway there is also deposition of C3d via the alternative pathway *in vivo*. We have not performed tissue staining for initiators of the lectin pathway such as MBL and ficolins but no binding of these molecules to IAPP could be detected in ELISA assays indicating that the lectin pathway is not triggered by IAPP amyloid. Interestingly, *in vitro* binding and deposition assays suggest that in addition to IAPP fibrils also non-fibrillar IAPP as the one found in rat can trigger some degree of complement activation.

Amyloid deposits can be very extensive and replace all the β-cells in an islet without overt signs of inflammation (41). This might at least in part be explained by the significant binding of the complement inhibitors C4BP and FH to the IAPP fibrils thus attenuating complement activation and inflammation. C4BP enhanced fibril formation by facilitating faster aggregation of IAPP. We hypothesize that by doing so C4BP minimizes the presence of cytotoxic oligomers of IAPP or perhaps in parallel the binding of C4BP to the IAPP oligomers could directly block their cytotoxic effect. We have previously found that C4BP bound equally well to mature fibrils and oligomers of prion protein (21). Certainly one cannot exclude that the binding of C4BP to IAPP has additional physiological functions. It is possible that complexes between C4BP and IAPP amyloid are already formed inside the β-cells. Expression databases report that C4BP is mainly expressed in liver hepatocytes then in the lung but also in pancreatic β-cells (42).

In conclusion, we propose that IAPP deposited in pancreas in the form of amyloid causes limited complement activation *in vivo*. These results are supported by *in vitro* findings. Furthermore, complement inhibitor C4BP is bound in large quantities to IAPP in pancreatic islets limiting complement activation. Another function of C4BP appears to be neutralization of cytotoxic oligomers of IAPP due to its ability to enhance fibril formation.

REFERENCES

1. Westermark, P., Wernstedt, C., Wilander, E., Hayden, D. W., O'Brien, T. D., and Johnson, K. H. (1987) *Proc Natl Acad Sci U S A* **84**, 3881-3885
2. Lukinius, A., Wilander, E., Westermark, G. T., Engstrom, U., and Westermark, P. (1989) *Diabetologia* **32**, 240-244
3. Kahn, S. E., D'Alessio, D. A., Schwartz, M. W., Fujimoto, W. Y., Ensinck, J. W., Taborsky, G. J., Jr., and Porte, D., Jr. (1990) *Diabetes* **39**, 634-638
4. Butler, A. E., Janson, J., Bonner-Weir, S., Ritzel, R., Rizza, R. A., and Butler, P. C. (2003) *Diabetes* **52**, 102-110
5. Maloy, A. L., Longnecker, D. S., and Greenberg, E. R. (1981) *Hum Pathol* **12**, 917-922
6. Jurgens, C. A., Toukatly, M. N., Fligner, C. L., Udayasankar, J., Subramanian, S. L., Zraika, S., Aston-Mourney, K., Carr, D. B., Westermark, P., Westermark, G. T., Kahn, S. E., and Hull, R. L. (2011) *Am J Pathol* **178**, 2632-2640
7. Guardado-Mendoza, R., Davalli, A. M., Chavez, A. O., Hubbard, G. B., Dick, E. J., Majluf-Cruz, A., Tene-Perez, C. E., Goldschmidt, L., Hart, J., Perego, C., Comuzzie, A. G., Tejero, M. E., Finzi, G., Placidi, C., La Rosa, S., Capella, C., Halff, G., Gastaldelli, A., DeFronzo, R. A., and Folli, F. (2009) *Proc Natl Acad Sci U S A* **106**, 13992-13997
8. Glabe, C. G. (2008) *J Biol Chem* **283**, 29639-29643
9. Rumora, L., Hadzija, M., Barisic, K., Maysinger, D., and Grubiic, T. Z. (2002) *Biol Chem* **383**, 1751-1758
10. Anguiano, M., Nowak, R. J., and Lansbury, P. T., Jr. (2002) *Biochemistry* **41**, 11338-11343
11. Zraika, S., Hull, R. L., Verchere, C. B., Clark, A., Potter, K. J., Fraser, P. E., Raleigh, D. P., and Kahn, S. E. (2010) *Diabetologia* **53**, 1046-1056
12. Ricklin, D., Hajishengallis, G., Yang, K., and Lambris, J. D. (2010) *Nat Immunol* **11**, 785-797
13. Klegeris, A., and McGeer, P. L. (2007) *Biochem Biophys Res Commun* **357**, 1096-1099
14. Walport, M. J. (2001) *N Engl J Med* **344**, 1058-1066
15. Sjoberg, A. P., Trouw, L. A., and Blom, A. M. (2009) *Trends Immunol* **30**, 83-90
16. Ziccardi, R. J., and Tschopp, J. (1982) *Biochem Biophys Res Commun* **107**, 618-623
17. Spitzer, D., Mitchell, L. M., Atkinson, J. P., and Hourcade, D. E. (2007) *J Immunol* **179**, 2600-2608
18. Akiyama, H., Barger, S., Barnum, S., Bradt, B., Bauer, J., Cole, G. M., Cooper, N. R., Eikelenboom, P., Emmerling, M., Fiebich, B. L., Finch, C. E., Frautschy, S., Griffin, W. S., Hampel, H., Hull, M., Landreth, G., Lue, L., Mrak, R., Mackenzie, I. R., McGeer, P. L., O'Banion, M. K., Pachter, J., Pasinetti, G., Plata-Salaman, C., Rogers, J., Rydel, R., Shen, Y., Streit, W., Strohmeyer, R., Tooyoma, I., Van Muiswinkel, F. L., Veerhuis, R., Walker, D., Webster, S., Wegrzyniak, B., Wenk, G., and Wyss-Coray, T. (2000) *Neurobiol Aging* **21**, 383-421
19. Hillarp, A., and Dahlback, B. (1990) *Proc Natl Acad Sci U S A* **87**, 1183-1187
20. Dahlback, B., and Stenflo, J. (1981) *Proc Natl Acad Sci U S A* **78**, 2512-2516
21. Sjoberg, A. P., Nystrom, S., Hammarstrom, P., and Blom, A. M. (2008) *Mol Immunol* **45**, 3213-3221
22. Trouw, L. A., Nielsen, H. M., Minthon, L., Londos, E., Landberg, G., Veerhuis, R., Janciauskiene, S., and Blom, A. M. (2008) *Mol Immunol* **45**, 3649-3660
23. Mollnes, T. E., Song, W. C., and Lambris, J. D. (2002) *Trends Immunol* **23**, 61-64
24. Dahlbäck, B. (1983) *Biochemical Journal* **209**, 847-856
25. Blom, A. M., Kask, L., and Dahlback, B. (2003) *Mol Immunol* **39**, 547-556
26. Tenner, A. J., Lesavre, P. H., and Cooper, N. R. (1981) *J Immunol* **127**, 648-653
27. Paques, E. P., Huber, R., Priess, H., and Wright, J. K. (1979) *Hoppe Seylers Z Physiol Chem* **360**, 177-183

28. Reid, K. B. (1976) *Biochem J* **155**, 5-17
29. Blom, A. M., Kask, L., and Dahlback, B. (2001) *J Biol Chem* **276**, 27136-27144
30. Garcia de Frutos, P., Hardig, Y., and Dahlback, B. (1995) *J Biol Chem* **270**, 26950-26955
31. Westermark, P., Engstrom, U., Johnson, K. H., Westermark, G. T., and Betsholtz, C. (1990) *Proc Natl Acad Sci U S A* **87**, 5036-5040
32. Betsholtz, C., Christmansson, L., Engstrom, U., Rorsman, F., Svensson, V., Johnson, K. H., and Westermark, P. (1989) *FEBS Lett* **251**, 261-264
33. Larsson, A., Soderberg, L., Westermark, G. T., Sletten, K., Engstrom, U., Tjernberg, L. O., Naslund, J., and Westermark, P. (2007) *Biochem Biophys Res Commun* **361**, 822-828
34. Manders, E. M., Stap, J., Brakenhoff, G. J., van Driel, R., and Aten, J. A. (1992) *J Cell Sci* **103 (Pt 3)**, 857-862
35. Pitsavos, C., Tampourlou, M., Panagiotakos, D. B., Skoumas, Y., Chrysohoou, C., Nomikos, T., and Stefanadis, C. (2007) *Rev Diabet Stud* **4**, 98-104
36. Ebeling, P., Teppo, A. M., Koistinen, H. A., and Koivisto, V. A. (2001) *Metabolism* **50**, 283-287
37. Kohl, J. (2006) *Curr Opin Mol Ther* **8**, 529-538
38. Webster, S., Bonnell, B., and Rogers, J. (1997) *Am J Pathol* **150**, 1531-1536
39. Head, E., Azizeh, B. Y., Lott, I. T., Tenner, A. J., Cotman, C. W., and Cribbs, D. H. (2001) *Neurobiol Dis* **8**, 252-265
40. Rostagno, A., Revesz, T., Lashley, T., Tomidokoro, Y., Magnotti, L., Braendgaard, H., Plant, G., Bojsen-Moller, M., Holton, J., Frangione, B., and Ghiso, J. (2002) *J Biol Chem* **277**, 49782-49790
41. Jaikaran, E. T., and Clark, A. (2001) *Biochim Biophys Acta* **1537**, 179-203
42. Hulbert, E. M., Smink, L. J., Adlem, E. C., Allen, J. E., Burdick, D. B., Burren, O. S., Cassen, V. M., Cavnor, C. C., Dolman, G. E., Flamez, D., Friery, K. F., Healy, B. C., Killcoyne, S. A., Kutlu, B., Schuilenburg, H., Walker, N. M., Mychaleckyj, J., Eizirik, D. L., Wicker, L. S., Todd, J. A., and Goodman, N. (2007) *Nucleic Acids Res* **35**, D742-746

FOOTNOTES

The authors would also like to acknowledge the expert technical help of Frida Mohlin, generous gift of antibodies detecting ficolins from prof. Garred (Copenhagen University, Denmark) and the financial support of the Swedish Research Council (2009-68X-14928-06-3 and 2010-55X-20326-04-3), the Swedish Foundation for Strategic Research, Swedish Diabetes Foundation and the Foundations of Österlund, Greta and Johan Kock, Family Ernfors, Knut and Alice Wallenberg and Inga-Britt and Arne Lundberg as well as grants for clinical research from the University Hospital in Malmö and the Region Skåne.

List of abbreviations: Aβ, amyloid-β; C4BP, C4b-binding protein; CCP, Complement control protein; FH, Factor H; HRP, horseradish peroxidase; IAPP, Islets amyloid polypeptide; MAC, Membrane attack complex; MBL, Mannose binding lectin; NHS, normal human serum; Tht, Thioflavin T; T2D, Type 2 diabetes;

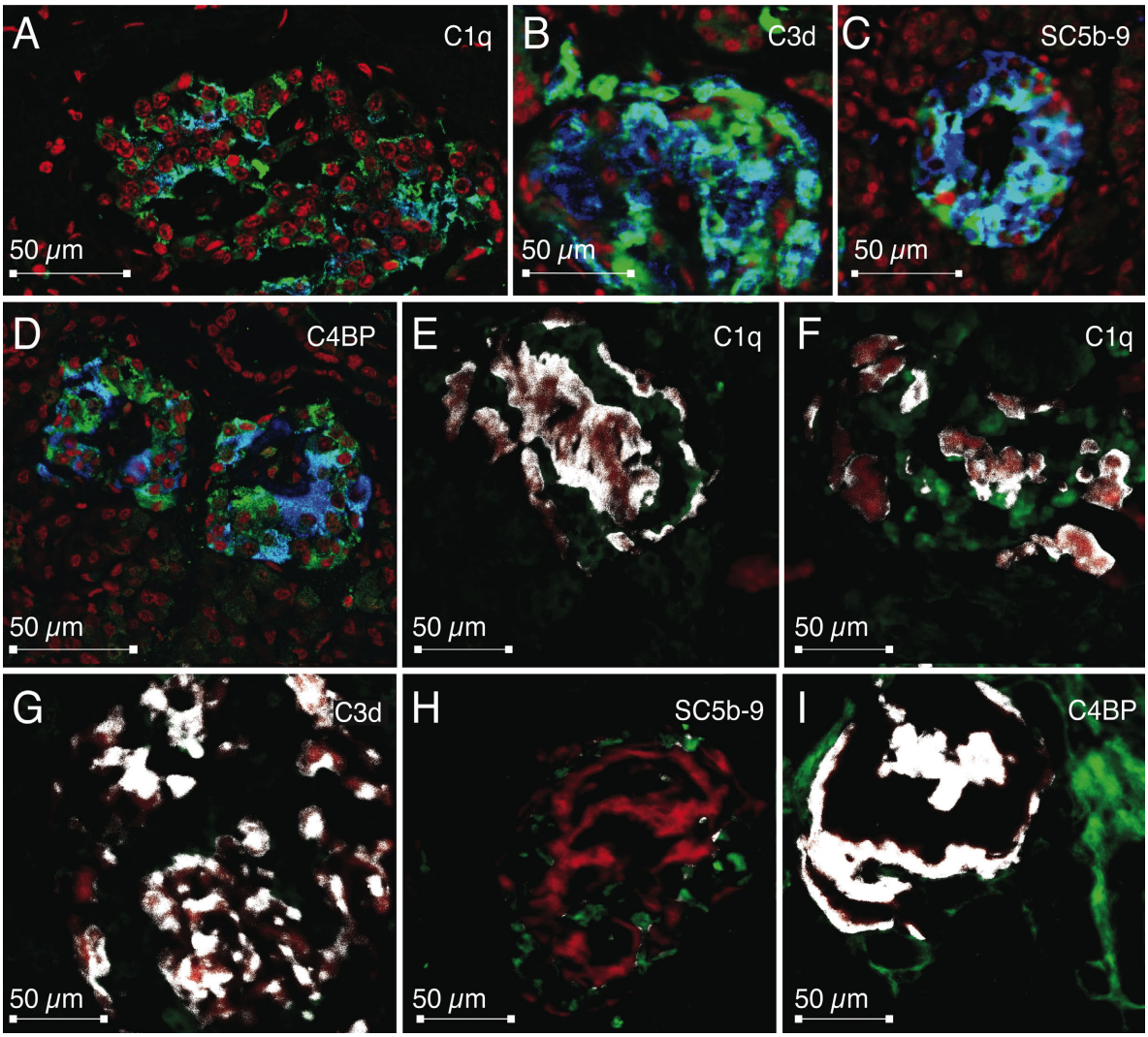

Figure 1 Complement components co-localize with IAPP deposits in pancreatic tissue. Formalin fixed sections of pancreatic tissue from T2D patients were stained with antibodies against IAPP (A-D), C1q (A), C3d (B), C5b-9; MAC (C) and C4BP (D). The complement factors were visualized using specific antibodies followed by secondary anti-rabbit antibodies conjugated with Alexa Fluor 488 (green) and the IAPP was visualized using secondary anti-mouse antibodies conjugated with Alexa Fluor 647 (blue). Colocalisation is indicated by presence of pale blue color. IAPP amyloid was in turn stained with Congo red (E-I) followed by detection of complement components C1q (E-F), C3d (G), C5b-9; MAC (H) and C4BP (I) with specific antibodies followed by secondary antibodies labeled with Alexa Fluor 488. Overlapping pixels were visualized as white using the ColocalizerPro software. The pictures were taken with a Zeiss LCM 510 confocal microscope at 40x magnification.

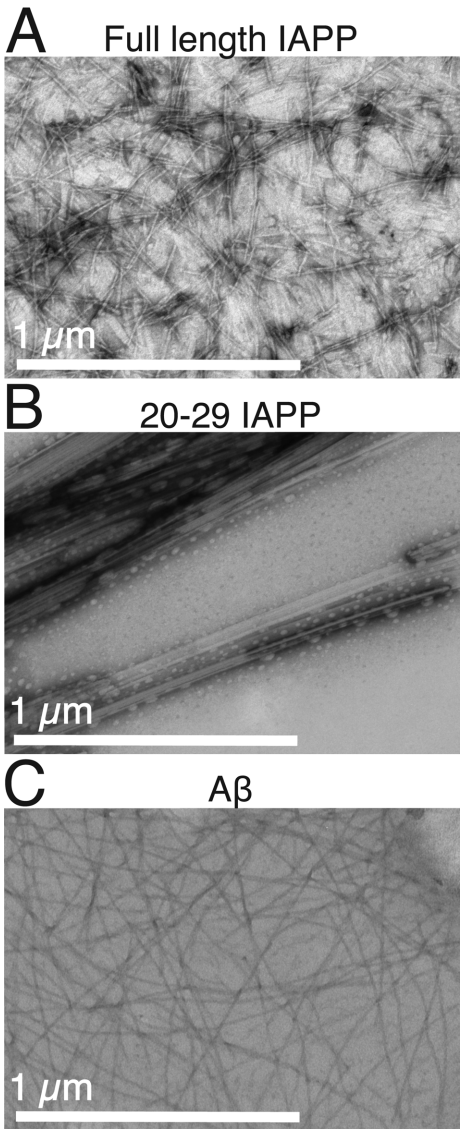

Figure 2 Visualization of IAPP fibrils formed *in vitro*. Panels show successful fibril formation for full length IAPP (A), 20-29 IAPP (B) and Aβ (C) visualized by electron microscopy. The presented images are representative of three separate experiments.

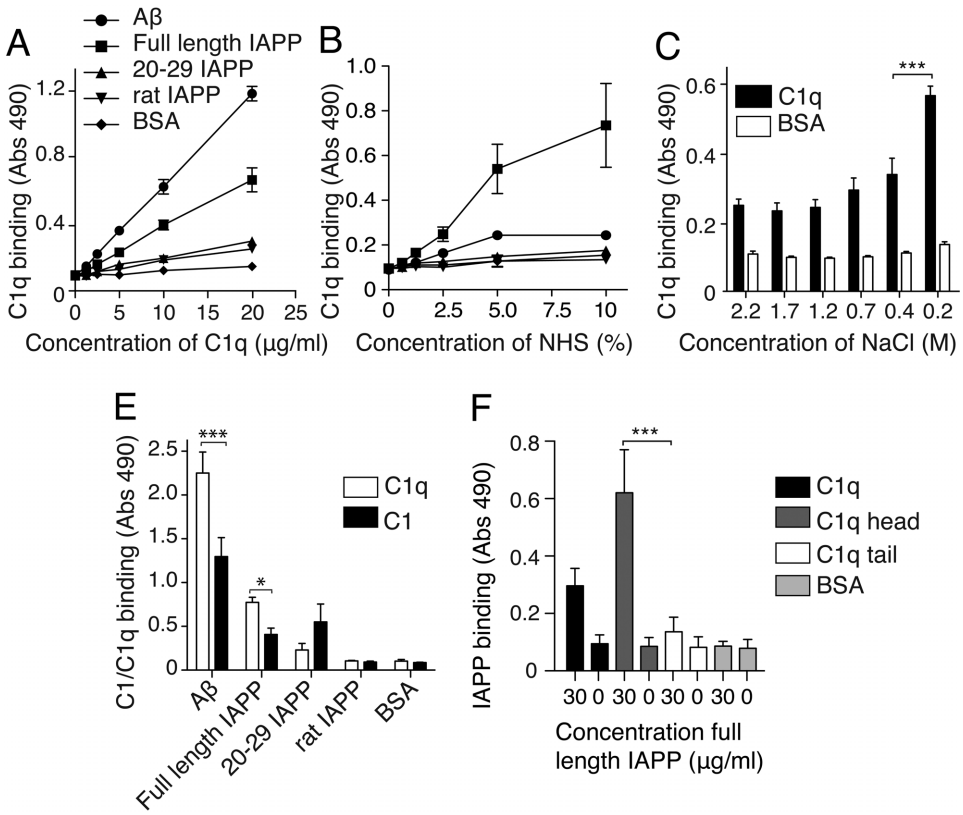

Figure 3 IAPP binds head domains of C1q. In panels A and B, IAPP variants were coated on the microtiter plate and in the fluid phase purified C1q (A) or NHS (B) were added in increasing concentrations followed by detection of bound C1q with antibodies. Purified C1q bound to IAPP in a concentration dependent manner with full length IAPP showing strongest binding (A). C1q/C1 from NHS bound only to full length IAPP (B). The binding between purified C1q (10 μg/ml) and full length IAPP is dependent on ionic interactions as the interaction was inhibited with increasing NaCl concentrations added to the binding buffer (C). When purified C1q and C1 complex (both at 50 μg/ml) were incubated with immobilized IAPP, C1q showed stronger binding then C1 (D). Immobilized C1q, C1q head and C1q tail fragments 10 μg/ml were incubated with 30 μg/ml IAPP and only purified C1q and C1q heads showed significant binding detected by polyclonal anti IAPP antibody (E). In panels A-D Aβ was used as a positive control. In panels A-E BSA was used as negative control. The results are given as means ± standard deviation (SD) for at least three independent experiments. ANOVA analyses were used for all the statistical evaluations. In panel A, all IAPP variants and Aβ, at a concentration of 20 μg/ml, showed a statistically significant binding compared to BSA. In Panel B full length IAPP was the only protein showing a statistically significant difference in binding compared to BSA at 2.5, 5.0 and 10.0% serum concentrations. In Panel C we noted statistically significant differences for all NaCl concentrations (*** $p<0.001$) when compared with the physiological NaCl concentration (0.15 M). In Panel D statistically significant differences were found for Aβ (*** $p<0.001$) and full length IAPP (* $p<0.05$) compared with BSA in regards to binding of both C1 and C1q.

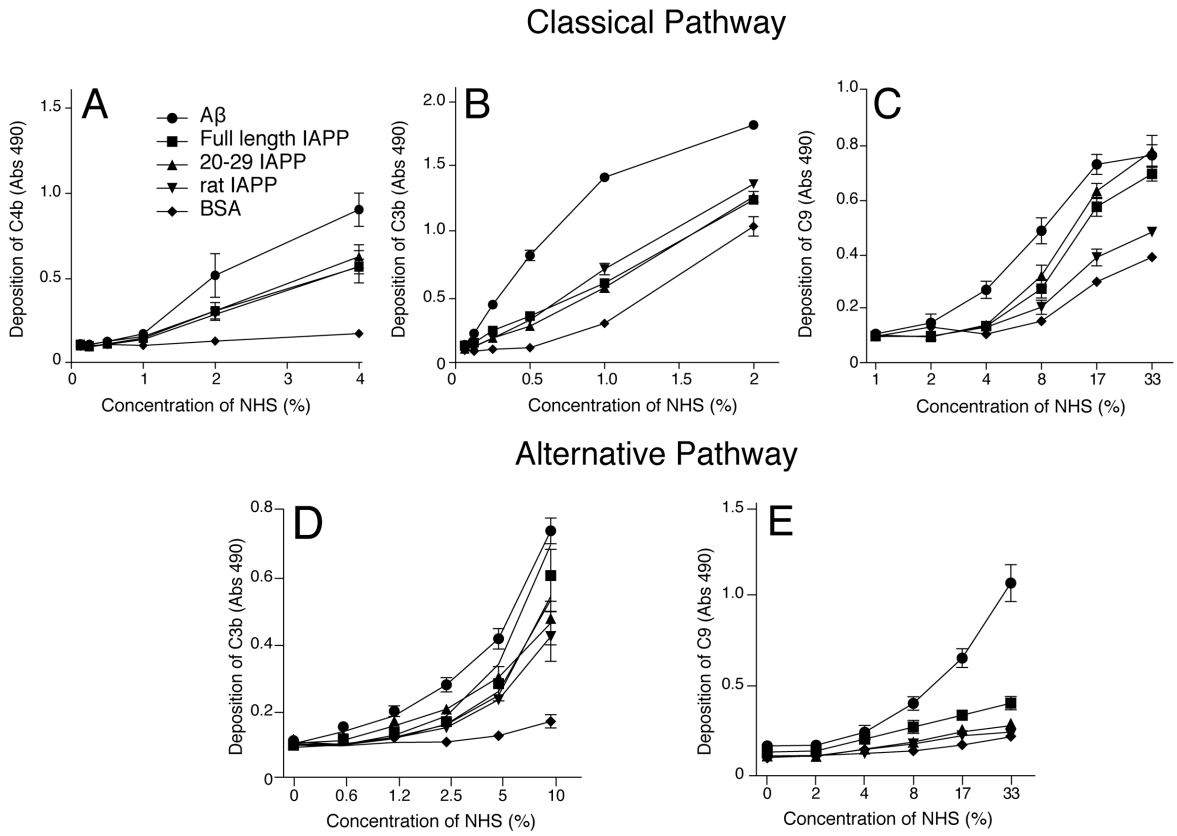

Figure 4 The IAPP variants trigger limited complement activation via the classical and the alternative pathways. IAPP variants were coated on microtiter plates and incubated with increasing concentrations of NHS diluted in GVB^{++} (classical pathway) or Mg-EGTA (alternative pathway). Aβ and BSA were used as a positive and a negative controls, respectively. Following complement activation, depositions of C4b (A), C3b (B, D) and C9 (C, E) were detected with specific antibodies. All IAPP variants triggered limited complement activation both through the classical (A-C) and the alternative pathway (D, E) most apparent at the level of C4b. The results are shown as means ± SD from three independent experiments. ANOVA analyses were used for the statistical evaluations. Panel A reveals statistically significant differences for Aβ, full length-, 20-29- and rat IAPP compared to BSA at both 2% and 4% serum. In panel B we obtained statistically significant differences for Aβ and all IAPP variants compared to BSA at both 1% and 2% serum. Panel C shows statistical significant differences for Aβ, full length-, 20-29- and rat IAPP compared to BSA at both 16.5% and 33% serum. In Panel D we obtained statistically significant differences for Aβ and all IAPP variants compared to BSA at both 5% and 10% serum. Panel E shows statistical significant differences for both Aβ and full length IAPP at both 16.75% and 33% serum.

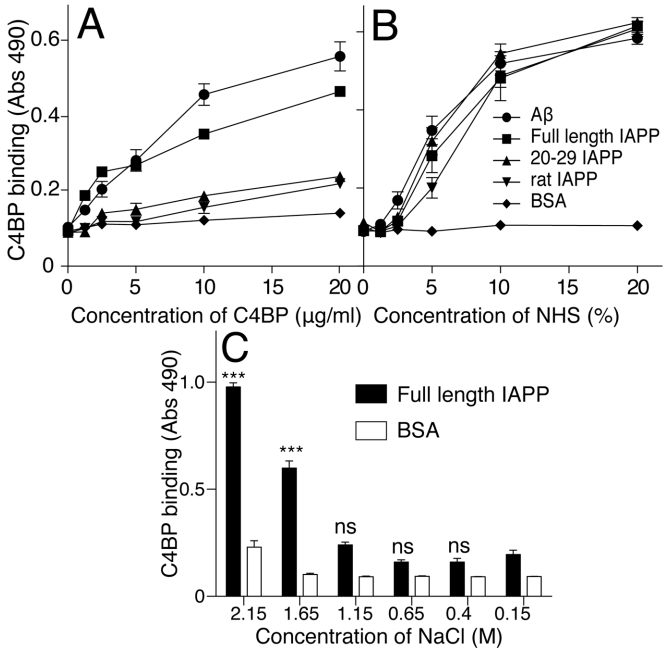

Figure 5 IAPP binds complement inhibitor C4BP. Increasing concentrations of purified C4BP (A) or NHS (B) were incubated with immobilized IAPP variants as well as Aβ and BSA and the binding was detected with specific antibodies. Purified C4BP bound mainly full length IAPP while C4BP from serum interacted with all IAPP forms with equal apparent affinity. The interaction between purified C4BP (10 μg/ml) and full length IAPP increased several fold at high NaCl concentrations implying that it is based on hydrophobic interactions. The results are presented as means ± SD for three independent experiments. ANOVA analyses were used for all the statistical evaluations. Panel A shows statistically significant differences for Aβ, full length, 20-29-, rat IAPP compared to BSA at 20 μg/ml of C4BP. Panel B reveals that Aβ, full length, 20-29-, rat IAPP exhibit statistically significant differences in binding compared to BSA at 10% and 20% of serum. In Panel C we noted statistically significant differences for 1.65 M and 2.15 M NaCl compared to the physiological NaCl concentration (0.15 M); (*** $p<0.001$).

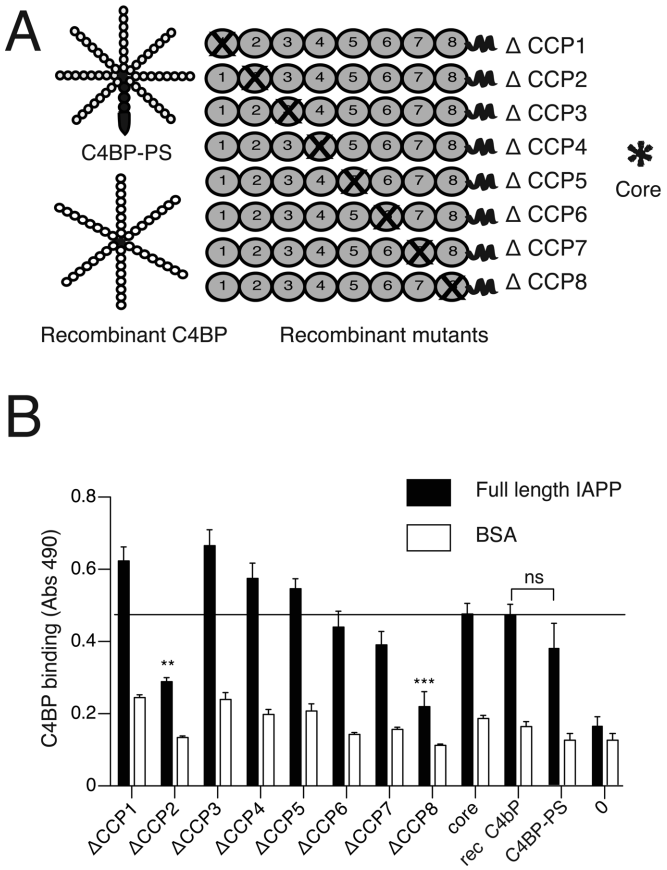

Figure 6 The C4BP domains CCP2 and CCP8 of α-chain bind IAPP. A) a schematic representation of the different C4BP variants used in this study. The predominant form of C4BP found in plasma is composed of 7 α-chains and one β-chain with bound protein S. The recombinant C4BP lacks both β-chain and protein S but retains capacity to inhibit complement. "Core" was prepared by digestion with chymotrypsin and contains the C-terminal polymerization region of C4BP with CCP8 and part of CCP7 domain. The panel also outlines the recombinant deletion mutants of C4BP that lack indicated CCP domains. B) All C4BP variants were incubated at 10 μg/ml with immobilized full length IAPP and the binding was detected with polyclonal antibody. BSA was used as a negative control. The recombinant wt C4BP bound well to IAPP indicating that the binding site is localized to the α-chain. CCP2 and CCP8 were required for the interaction and the presence of binding site in the C-terminus of C4BP was confirmed by binding of the core to IAPP. The results are presented as means ± SD for three independent experiments. Panel B shows statistically significant differences for the deletion mutants CCP2 (** $p<0.01$) and CCP8 (*** $p<0.001$) compared to wt C4BP using ANOVA analysis; ns – not significant.

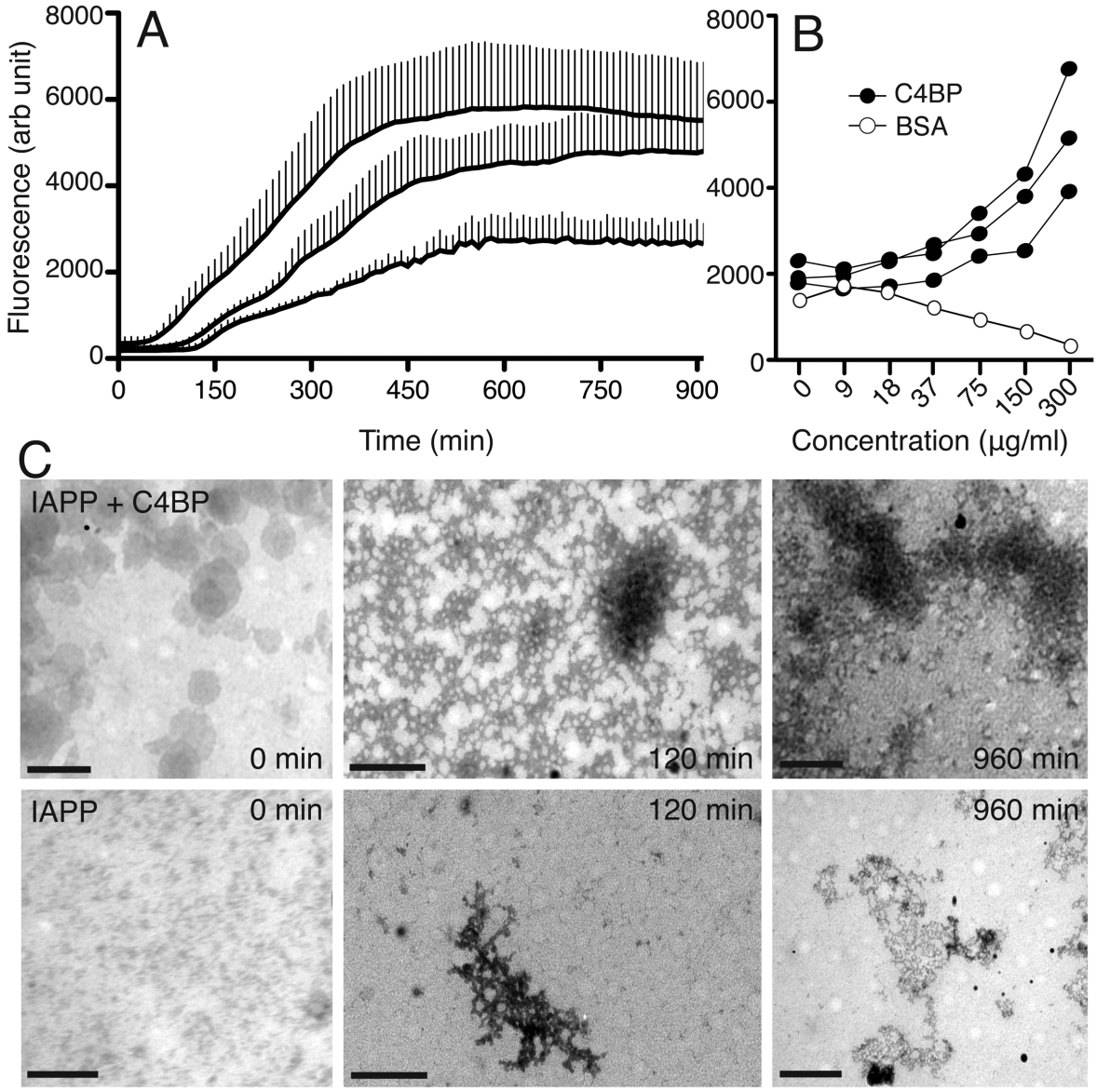

Figure 7 C4BP-mediated modulation of the kinetics of IAPP aggregation. Panel A, the kinetics of the IAPP fibril formation in the presence of Tht and C4BP (concentrations ranging from 18 – 300 µg/ml with curves obtained for only 150 and 300 µg/ml of C4BP shown in the figure for clarity). The results are presented as means ± SD for three independent experiments. There was a significant increase of the amount of fibril formation in the presence of 75 (* $p < 0.05$, not shown), 150 (** $p < 0.001$) and 300 µg/ml C4BP (*** $p < 0.0001$) compared with IAPP alone estimated using two way ANOVA analysis with Bonferroni post-test at the end point. Addition of 38 µg/ml or less of C4BP did not significantly alter the fibril formation. Panel B shows the effects of different C4BP concentrations in the individual experiments at fixed time point of 400 min. BSA, the negative control did not enhance fibril formation at any concentration tested. In C, upper panel shows EM pictures depicting IAPP fibril formation in the presence of 300 µg/ml C4BP, analyzed at time points 0, 120 and 960 min and lower panel shows EM pictures from IAPP fibril formation at the same time points. Extensive amounts of small fibrilar aggregates were abundantly detected on all analyzed grids in the presence of C4BP already at time point 120 minutes and aggregate size increased with time. In samples from aggregating IAPP alone there were only few aggregates detected, examples of such aggregates detected at 120 and 960 min are shown. Bars correspond to 200 nm.

Table 1. Colocalization between IAPP and complement components, using Manders correlation coefficient, R. R can vary from 0 to 1 and value of 0.5 implies that 50% of both channels colocalize. Congo red staining detects IAPP amyloid and the antibody recognizes all intracellular and extracellular forms of IAPP.

Complement protein	Congo red staining	IAPP antibody
C1q	R= 0.33 ± 0.13	R=0.66 ±0.13
C3d	R= 0.71 ± 0.09	R=0.64 ± 0.04
SC5b-9 (MAC)	R= 0.15 ± 0.14	R=0.77 ± 0.04
FH	R= 0.48 ± 0.06	R=0.65 ± 0.17
C4BP	R=0.77 ± 0.02	R=0.69 ± 0.09

Supplementary material

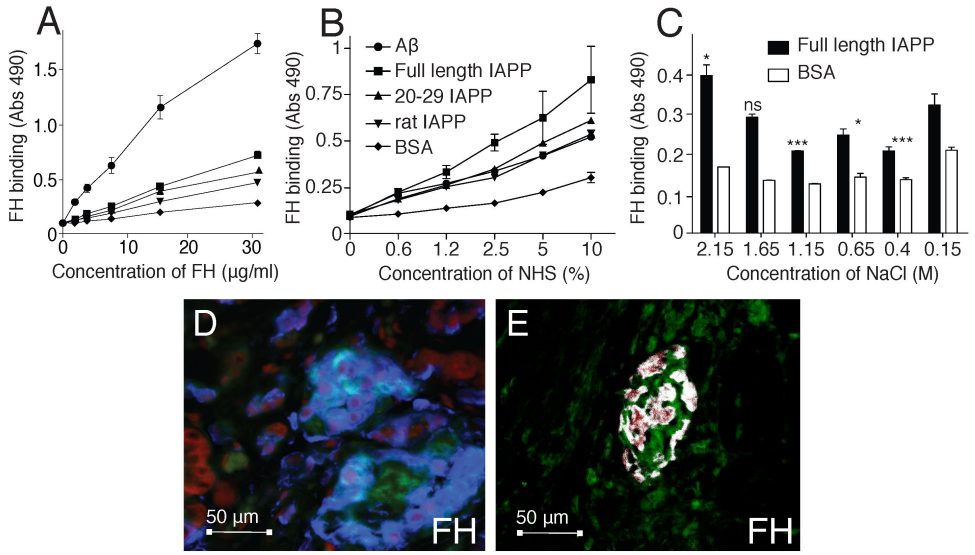

Supplementary Figure 1 IAPP binds complement inhibitor FH. Increasing concentrations of purified FH (A) or NHS (B) were incubated with immobilized IAPP variants as well as Aβ and BSA and the binding was FH was detected with specific antibodies. Purified FH bound mainly full length IAPP and so did the FH from serum. The interaction between purified FH (10 µg/ml) and full length IAPP increased at high NaCl concentrations implying that it is based on hydrophobic interactions. The results are presented as means ± SD for three independent experiments. ANOVA analyses wereused for all the statistical evaluations. Panel A shows statistically significant differences for Aβ, full length IAPP compared to BSA at 30 µg/ml of FH. Panel B reveals that Aβ, full length, 20-29-, rat IAPP exhibit statistically significant differences compared to BSA at 10% of serum. In Panel C we noted statistically significant differences for 2.65 M compared to the physiological NaCl concentration (0.15 M); (* $p<0.05$, *** $p<0.001$; ns – not significant). Panel D shows FH, which was visualized using specific antibodies followed by secondary anti-rabbit antibodies conjugated with Alexa647 (blue) and the IAPP was visualized using monoclonal antibody followed by secondary anti-mouse antibodies conjugated with Alexa488 (green). The lighter blue shows colocalization. Panel E; Mature fibrils of IAPP were stained with Congo red followed by detection of FH with specific antibodies (green). Overlapping pixels were visualized as white using the ColocalizerPro software. The pictures were taken with a Zeiss LCM 510 confocal at 63x magnification. The image is representative of three independent staining experiments.